Positron annihilation in helium- and krypton-decorated microvoids in fcc metals

P. Jena and B. K. Rao*
Department of Physics, Virginia Commonwealth University, Richmond, Virginia 23284
(Received 10 September 1984)

The electronic structure and positron annihilation characteristics (lifetime and angular correlation between annihilation quanta) in microvoids containing 1, 2, 4, 8, 10, and 13 vacancies in fcc Cu and Al have been calculated using the density-functional formalism and local-density approximation. The positron lifetimes and binding energies are shown to increase with the void size, saturating when voids become big. The positron lifetimes are found to drop sharply when these voids are decorated with rare-gas atoms such as He and Kr. The angular correlation curves are found to broaden when vacancies are decorated with rare-gas atoms with a concomitant decrease in the peak counting rate. The results are compared with recent experiments on He-irradiated Al and Kr-irradiated Cu. Comparison between theoretical and experimental positron lifetimes sheds light on the morphology of defects trapping the positrons. The technological significance of the present study is also pointed out.

I. INTRODUCTION

One of the important objectives in the study of materials science is to attain a fundamental understanding of the interaction of defects with host atoms. As experimental methods are becoming more sophisticated, it is increasingly apparent that the properties of defects are influenced not only by their interaction with host atoms, but also with other defects intrinsic to the host lattice. For example, voids created by the agglomeration of migrating vacancies during stage-III annealing may completely anneal out at higher temperatures. It has been found[1] that these voids may be stabilized at higher temperatures if they are decorated with helium. Similarly, the diffusion of hydrogen has been found[2] to be affected by its interaction with impurities and vacancies in a metal lattice. It is therefore worthwhile to understand the nature of interaction of hydrogen and rare-gas atoms with vacancy-type defects, since the trapping of one defect by another may have important technological consequences.

Numerous techniques (e.g., transmission electron microscopy, small-angle x-ray and neutron scattering, electron energy loss spectroscopy, uv optical absorption) are available to study the size of voids containing rare-gas atoms. The experimental resolution of many of these techniques, however, limit their usability for studying very small voids (i.e., voids of radius $\lesssim 10$ Å). One of the techniques which is particularly suitable to study the size of these small voids is the positron annihilation technique[3] (PAT).

The attraction of positrons to vacancylike defects has established PAT as a sensitive probe of defects. In a perfect metal, the repulsion of a positron from the ion core makes it sample the interstitial region of the lattice. The lifetime of the positron in the bulk is then determined by the interstitial electron density. For a metal containing a vacancy, the positron, on the other hand, usually finds itself trapped in the vacancy. Since the density of electrons inside a vacancy is always less than that in the interstitial region, the lifetime of a vacancy-trapped positron is larger than that of the positron annihilating in the free state. As vacancies cluster to form voids, the binding energy and lifetime of positrons increase with increasing void size. Since a large void can be considered as an internal surface, the positron lifetime saturates to a fixed value characteristic of the lifetime of a surface-state positron. This saturation typically occurs[4] when the void radius reaches a value of about 10 Å. Thus the lifetime of positrons inside small voids can provide a signature of the void size.

If voids are created by irradiating the material with rare-gas atoms such as helium and krypton, a significant number of voids may contain the rare-gas atom. The lifetime of a positron in a void decorated with a rare-gas atom is then expected to be shorter than that in a clean void of the same size. This is because positrons will be pushed out from the center of the void by the rare-gas atom and will sample a region of higher electron density.

To interpret the observed lifetime components in terms of defect morphology, theoretical input is necessary. To illustrate this point further, we briefly discuss a recent positron annihilation study[5] of copper containing a high concentration of krypton. Through transmission electron microscopy, Eldrup and Evans[5] observed a very high den-

TABLE I. Positron lifetimes in Cu.

Sample	Lifetime of positrons (ps)
Pure Cu	120
Thermally induced vacancies	167
Vacancies created by electron irradiation	180±10
Defect in deformed Cu	175–193
Irradiation-induced voids	300–600
Irradiated with Kr	260

sity of small cavities. However, lifetime experiments indicated that 90% of the positrons annihilate in this material with a single lifetime of 260 ps. To put this in perspective, we list in Table I characteristic lifetimes of positron in copper under various sample conditions. The results in Table I clearly indicate that if the positrons in the Eldrup-Evans experiment were annihilating in the large visible bubbles, the lifetimes would be much larger than the observed 260 ps. One, therefore, concludes that there are a large number of submicroscopic voids containing krypton which screen the visible bubbles from the positron. Unfortunately the positron annihilation experiments cannot, alone, reveal the size of the void and the density of krypton in the void in which the positrons are trapped. Thus theoretical calculations are necessary to find the dependence of the positron lifetime on void size and krypton density. A comparison of the calculated lifetimes with the experimental value can then isolate the defect complex trapping the positron in the irradiated sample. Similar information can also be obtained by comparing the angular correlation curves between photons produced during positron annihilation.

In the next section we discuss the various theoretical techniques commonly used in the study of positron lifetime. We compare the results derived from various model calculations and show that the positron lifetimes are not very sensitive to details in the calculations. In Sec. III we present results of positron lifetime calculations and angular correlation in clean as well as helium- and krypton-decorated microvoids of varying sizes in fcc Cu and Al. The results are compared with recent experimental data. Section IV contains a summary of our conclusions.

II. SURVEY OF THEORETICAL METHODS

The positron annihilation rate λ ($\lambda=1/\tau$) is given by

$$\lambda=\pi r_0^2 c \int d^3r n_+(\mathbf{r})\tilde{n}_-(\mathbf{r}) , \tag{1}$$

where $r_0=e^2/mc^2$ is the classical electron radius, e is the electron charge, and c is the speed of light. $n_+(\mathbf{r})$ is the density distribution of the positron and $\tilde{n}_-(\mathbf{r})$ is the density of the electron in the presence of the defects and the positron. Due to the mutual attraction between the electron and the positron the electron density around a positron is expected to be enhanced. Since a self-consistent treatment of the electrons interacting simultaneously with the defects and the positron is very difficult, one decouples these interactions by using a local-density approximation to account for the electron-density enhancement at the positron site. For computational purposes, Eq. (1) is rewritten as

$$\lambda=\int d^3r n_+(\mathbf{r})\Gamma(n_-(\mathbf{r})) , \tag{2}$$

where Γ is a function of $n_-(\mathbf{r})$, the electron density in the absence of the positron. Since the electron density $n_-(\mathbf{r})$ in the imperfect lattice is composed of both free and bound core electrons, they are expected to be influenced differently by the presence of the positron. Thus $\Gamma(n_-(\mathbf{r}))$ is broken into two parts:[6]

$$\Gamma(n_-(\mathbf{r}))=\Gamma_v(n_v(\mathbf{r}))+\Gamma_c(n_c(\mathbf{r})) . \tag{3}$$

$n_v(\mathbf{r})$ and $n_c(\mathbf{r})$ are, respectively, the valence- and core-electron densities. In transition-metal hosts where d electrons are quasilocalized a third term $\Gamma_d(n_d(\mathbf{r}))$ may be added[6] to Eq. (3). The local rate of annihilation with valence electrons Γ_v is approximated by the Brandt-Reinheimer formula,[7]

$$\Gamma_v(n_v(\mathbf{r}))=(2+134n_v)\text{ns}^{-1} . \tag{4}$$

The local anninilation rate with the core electrons Γ_c calculated in the independent-particle approximation[8] is given by

$$\Gamma_c(n_c(\mathbf{r}))=\pi r_0^2 c\gamma_c n_c(\mathbf{r}) , \tag{5}$$

where $\gamma_c=1.5$ is a constant enhancement factor for core electrons.

In the case of impurity-decorated voids, two different core-electron types are involved—one corresponding to the impurity core electrons, the other corresponding to the host core electrons. In a jellium model for the host, the annihilation rate with the host core electrons can be included by replacing the electron density outside the void cell by $n(\mathbf{r})+(\Gamma_c^h/\Gamma_v)n_0$, where Γ_c^h is the annihilation rate with the host core electrons. We have used $\Gamma_c^h/\Gamma_v=0.154$ for Al and 2.16 for Cu which yield bulk lifetimes of 162 ps in Al and 137 ps in Cu. These values agree closely with the experimental values[9] of 161 ps in Al and 132 ps in Cu.

Experimental information on the electronic structure of defects can also be obtained from the study of angular correlation between photons produced during the annihilation event. We have calculated the electron wave function and density due to a void decorated with a rare-gas atom by representing the external perturbation as

$$n_{\text{ext}}(\mathbf{r})=A\delta(\mathbf{r})+n_0\Theta(\mathbf{r}-\mathbf{R}) , \tag{6}$$

where $\mathbf{R}$ is the radius of the void and n_0 is the average density of the positive-ion charge in the metal matrix. Θ is the usual Heaviside function. A is the atomic number of the rare-gas atom which is assumed to occupy the center of the void. This assumption is valid since the interaction between a metal atom and rare-gas atom is repulsive.

The response of the electrons to the external perturbation is calculated self-consistently by solving the Hohenberg-Kohn-Sham equation[10] in the local-density approximation, namely,

$$(-\nabla^2+V_{\text{eff}})\psi_i=\epsilon_i\psi_i . \tag{7}$$

The electron density n_- is given by

$$n_-(\mathbf{r})=\sum_{\substack{i\\ \text{occ}}} |\psi_i(\mathbf{r})|^2 . \tag{8}$$

The electrostatic potential Φ is obtained by solving the Poisson equation,

$$\nabla^2\Phi=-8\pi[n_-(r)-n_{\text{ext}}(r)] . \tag{9}$$

The effective potential in Eq. (7) is calculated by adding to Φ the exchange-correlation potential in the local-density approximation,

$$V_{\text{eff}}(\mathbf{r})=\Phi(r)+V_{\text{xc}}(n_-(\mathbf{r}))\ . \tag{10}$$

Equations (7)—(10) are solved self-consistently.

The positron wave function ψ_+ and the binding energy ϵ_b can be calculated by solving the Schrödinger equation for the positron,

$$[-\nabla^2+V_+(\mathbf{r})]\psi_+(\mathbf{r})=-\epsilon_b\psi_+(\mathbf{r})\ . \tag{11}$$

Only the bound-state solutions of Eq. (11) are of interest. Since there is only one positron at a time in the metal matrix, only the $1s$ bound state for the positron needs to be evaluated. The positron potential V_+ can be constructed using the pseudopotential picture of Stott and Kubica,[11]

$$V_+(\mathbf{r})=-\Phi(\mathbf{r})+V^{\text{corr}}(n_-(\mathbf{r}))-V^{\text{corr}}(n_0)$$
$$-V_0\Theta(\mathbf{R}-\mathbf{r})\ . \tag{12}$$

The correlation potential $V_+^{\text{corr}}(n_-(\mathbf{r}))$ for the positron with the electrons is calculated in the local-density approximation from the electron-gas data. The positron correlation energy for the background $V^{\text{corr}}(n_0)$ is subtracted so that the potential in Eq. (12) would vanish at infinity. V_0 is the kinetic energy of the positron in the perfect host[12] (4.9 eV in Al and 4.8 eV in Cu).

In the above method, the periodic structure of the host metal matrix is ignored. The ionic charges localized at lattice sites are smeared to form a homogeneous density of positive charges. This model, although not unreasonable for simple free-electron-like metals, does not apply to metals with complicated band structures such as transition metals. Its merit arises from the simplicity of the calculation procedure. As we shall show in the following, the quality of agreement of experimental with calculated values in the jellium model is as good as that obtained from other theoretical methods.[13–20]

Another situation one has to consider while calculating positron lifetimes in defect complexes is that the decorated defects may not provide a spherically symmetric positron potential $V_+(\mathbf{r})$. For example, in a hydrogen-vacancy complex, hydrogen, unlike the rare-gas atoms, may not be situated at the center of the vacancy. Thus the potential experienced by the electrons as well as positrons may not be spherically symmetric. Consequently, the respective Schrödinger equations (7) and (11) cannot be reduced to a simple one-dimensional radial form. Puska and Nieminen[6] recently suggested a new method which can take into account the nonspherical situation and yet provide a computationally simple procedure. In this method (referred to as the superposition-atom model) the electron density and Coulomb potential of the lattice containing any kind of defects are constructed by superimposing atomic charge densities and atomic potentials. The positron potential is constructed as outlined in Eq. (12) and the positron wave function is obtained by solving the three-dimensional Schrödinger equation (11) using the "finite elements" technique. Thus the superposition-atom model and jellium model, described earlier, represent two extreme points of view. In the jellium model the discrete nature of the host lattice and nonspherical nature of decorated defects are ignored while the perturbations on the electron density and potential caused by the defects are treated self-consistently. In the superposition-atom model, on the other hand, the discreteness of the host lattice is fully taken into account while the ambient electron density is not allowed to be readjusted because of the defect. We should point out that by superimposing atomic densities, one does achieve a reasonable approximation to the vacancy density. A further limitation of the superposition model is that the knowledge of electron wave functions is lost. Thus one cannot calculate the angular correlation curve using this approach.[6]

Alternate methods based on "supercell" band-structure calculations[16,17] and the molecular-cluster method[18] do exist where the discrete nature of the host lattice, charge perturbation caused by the defects, and nonspherical nature of decorated defects can all be taken into account. These methods, however, make substantial demand on computer time and cannot conveniently be used for systematic analyses designed to predict defect morphology. This aspect will be illustrated in the next section. Another disadvantage of these methods is that computational time considerations limit the size of the supercell and the cluster. Consequently it is difficult to apply these methods to large voids and bubbles.

In order to appreciate the advantages of the simpler theoretical models and to facilitate the discussion of the results in the next section we provide a survey of the computed positron lifetimes and binding energies using various theoretical approaches for various defects in Al in Table II. It is clear that all the computed lifetimes are in good agreement with each other and with experiment. The positron binding energies, on the other hand, are sensitive to approximations in theoretical models. The lack of sensitivity of positron lifetimes arises from the fact that the annihilation rate in Eq. (2) is an integrated quantity and includes contributions from a large region surrounding the defect. Thus the computed positron lifetimes for various voids and bubbles using the jellium model presented in this paper are believed to be accurate and can be used to illustrate defect morphology. This is the subject for discussion in the following section.

III. RESULTS AND DISCUSSIONS

We have calculated the electronic structure and positron lifetimes in vacancy clusters containing 1, 2, 4, 8, 10, and 13 vacancies in fcc Al and Cu. The calculations have been repeated by placing at the center of the cluster helium and krypton atoms. We first discuss the results in the Cu host.

In Figs. 1(a), 2(a), and 3(a) we have plotted the electron-density distributions around an 8-atom void and 8-atom voids containing a He or a Kr atom at the center, respectively. The depletion of electron density from inside the void due to the removal of the positive-ion core of the host is clearly visible in Fig. 1(a). When rare-gas atoms such as He and Kr occupy the void center there is a sharp increase in the electron density at the center of the void. The density of electrons at the center of the Kr—8-atom-void [Fig. 3(a)] complex is much larger than that in the case of He—8-atom-void [Fig. 2(a)] complex since the atomic number of Kr is 36 while that of He is only 2. Furthermore, the electron density in Kr-decorated void is

TABLE II. Calculated positron lifetimes τ and binding energies ϵ_b in defects in Al.

Defect	Model	Reference	τ (ps)	ϵ_b (eV)
Monovacancy	Density-functional			
	jellium	15,4	243	1.75
	Supercell augmented			
	plane wave	16	231	3.31
	Supercell			
	pseudopotential	17	250	2.17
	Superposition-atom	6	253	2.30
	Molecular-cluster	18	248	1.51
	Expt.	9	241	
Divacancy	Spherical jellium	19	264	3.19
	Elliptical jellium	19	257	2.60
	Superposition-atom	6	273	3.30
	Supercell	17	285	2.98
Vacancy-hydrogen complex	Jellium	21	188	1.61
	Superposition-atom	6	204	1.40
	Molecular-cluster	18	191	0.47

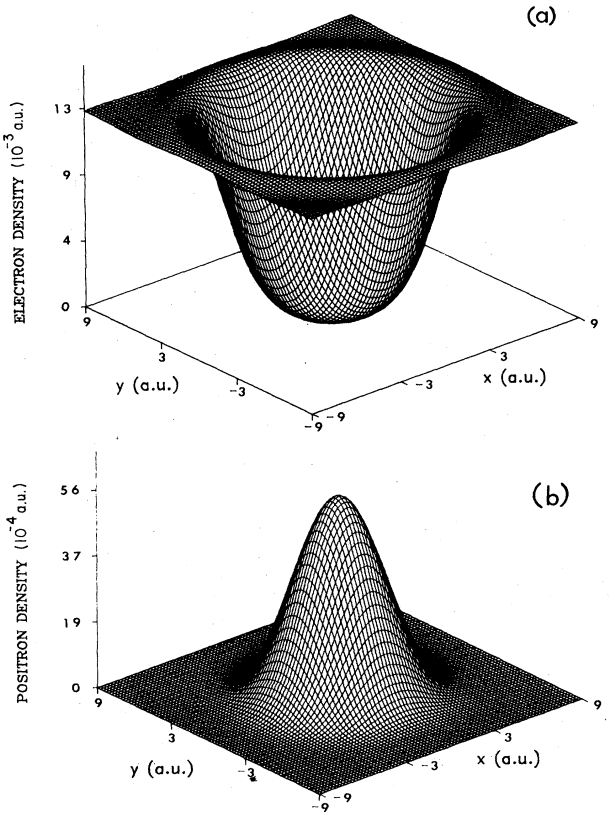

FIG. 1. (a) Electron density and (b) positron density distribution around an eight-atom void in Cu.

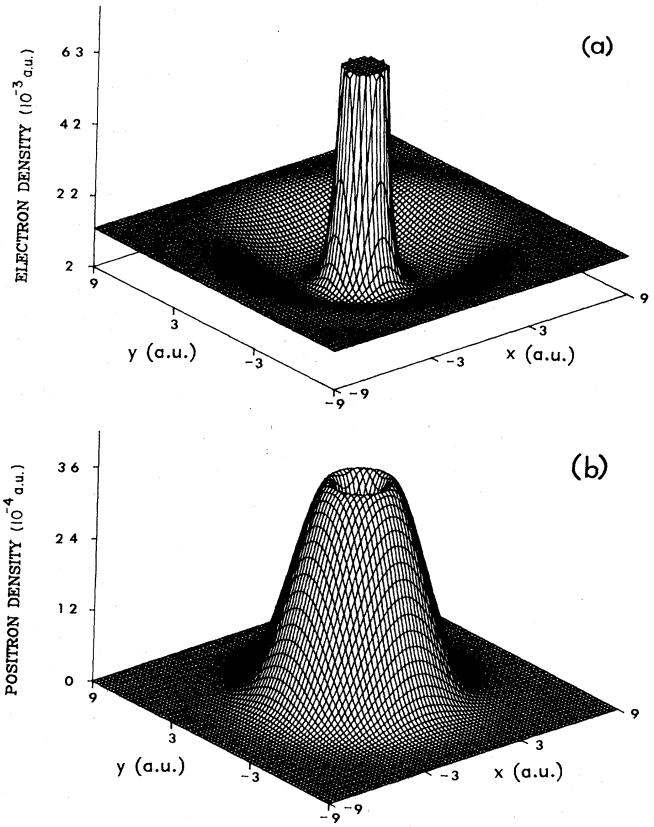

FIG. 2. (a) Electron density and (b) positron density distribution around an eight-atom void containing a He atom at its center in Cu.

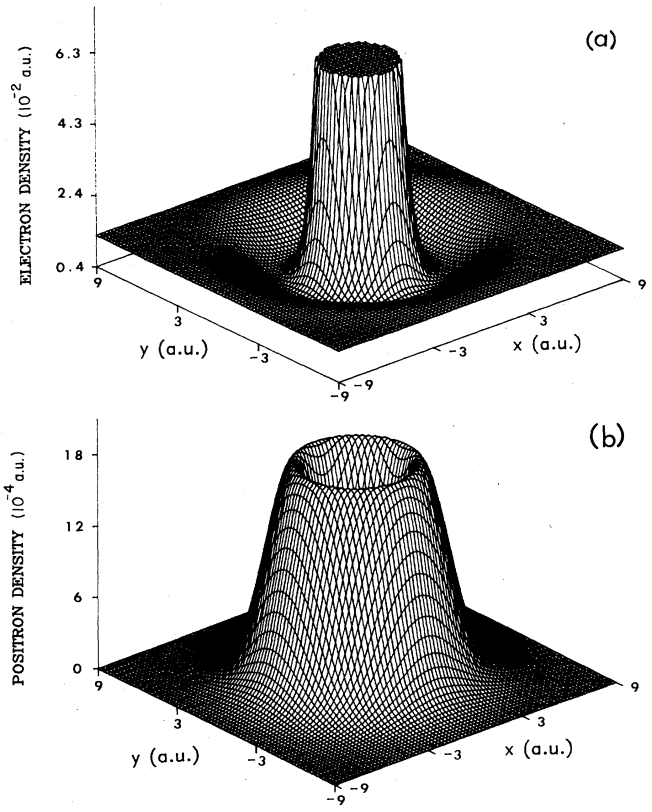

FIG. 3. (a) Electron density and (b) positron density distribution around an eight-atom void containing a Kr atom at its center in Cu.

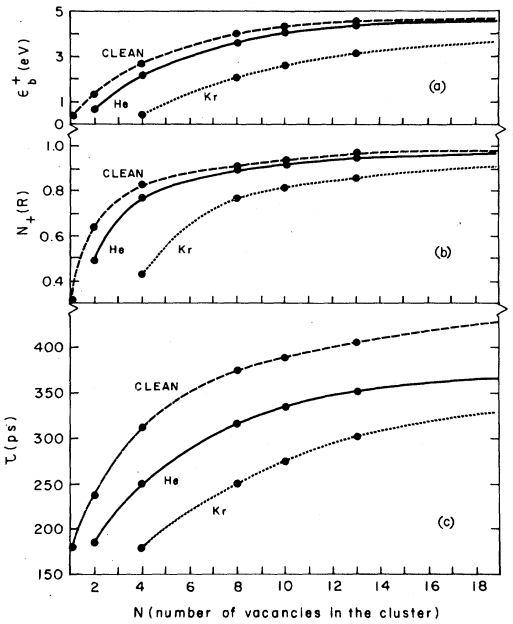

FIG. 4. Variation of (a) positron binding energy, (b) positron fraction inside the void, and (c) positron lifetime with void size in Cu. In each case, the dashed curve corresponds to clean void, solid curve corresponds to voids decorated with He, and dotted curve corresponds to voids decorated with Kr.

much more spread out than that decorated with He. In Figs. 1(b), 2(b), and 3(b), we plot the corresponding positron density distributions. The behavior of the positron is opposite to that of the electron. The positron was found to be trapped by the void and its binding energy decreased steadily from its value in the clean void to its value in those decorated by He and Kr. The "hole" in the positron density distribution in Fig. 2(b) and 3(b) signifies the repulsion of the positron from the positive-ion cores of the rare-gas atoms. The size of the holes is related to the size of the rare-gas atoms.

The binding energies of the positron in rare-gas-atom-decorated vacancy complexes depend on the size of the vacancy complexes as well as the atomic number of the impurities decorating the void. For example, a monovacancy of Cu containing a He atom is unable to trap positrons. For these impurity-vacancy complexes, positrons cannot be used as probes. In Fig. 4 we plot the variation of the positron binding energy with void size for clean as well as He- and Kr- decorated voids in Cu. Two distinct features are apparent. First, the binding energy increases with void size. This increase is more rapid when vacancy clusters are small in size and appears to saturate as voids become large. This saturation is characteristic of the large voids mimicking an internal surface. The increase in binding with increasing void size arises from the removal of positive host-ion cores [see Eq. (12)] from the lattice. Secondly, as the voids become decorated with impurities the binding energy of positrons starts to decrease due to the repulsion from the impurity core. The binding energy of the positron in a Kr-decorated void is less than a He-decorated void of the same size.

With increasing binding energy the positron becomes more localized. Thus the fraction of positrons inside a void increases and approaches unity as the void grows in size. Since a positron localized inside a void has less of a chance to annihilate with the core electrons of the host-metal atoms, the approximation discussed in the preceding section for the role of host core electrons on positron annihilation would not influence the predicted lifetimes in large voids. The lifetimes of positrons in clean as well as decorated voids are shown in Fig. 4(c). It is clear that the lifetimes are dependent on the void size as well as on the nature of the impurity decorating it. Thus the positron lifetimes can be used to probe the size and structure of defect complexes.

We now compare our results with the experiment of Eldrup and Evans.[5] As pointed out earlier, Eldrup and Evans observed that 90% of the positrons annihilated with a single lifetime of 260 ps. From our results in Fig. 4(c), this lifetime would originate from voids of nine vacancies containing a single Kr atom. In order to set a confidence limit on this assignment of defect structure, we compare in Table III the present positron binding energies and lifetimes in 4- and 13-vacancy clusters with those cal-

TABLE III. Positron binding energies and lifetimes calculated in the noninteracting model (Ref. 20) and jellium model (present calculation) in microvoids in Cu.

No. of vacancies in the cluster	Condition	Present result ϵ_b (eV)	Present result τ (ps)	Ref. 20 ϵ_b (eV)	Ref. 20 τ (ps)
4	Clean	2.75	311	3.7	280
	Kr-decorated	0.44	179	1.8	220
13	Clean	4.50	407	5.5	374
	Kr-decorated	3.17	302	4.6	290

culated by Hansen *et al.*[20] Our calculated binding energies are typically about 1.0 eV lower than that of Hansen *et al.* whereas our calculated lifetimes in Kr-decorated voids are in good agreement with their calculated values. Since a 13-atom void can be expected to be much closer to being spherical than the 4-atom void, we believe that the remaining discrepancy in the positron lifetime in a Kr—13-atom void calculated by us and by Hansen *et al.* could arise from the neglect of charge readjustment around a Kr—13-atom void by Hansen *et al.*[20] A calculation of positron annihilation involving the discrete structure of the defect complex as well as the charge relaxation will be necessary if one were to assign the 260-ps lifetime to a specific structure in a quantitative way. It is sufficient to say that the positron lifetime observed by Eldrup and Evans originates from the annihilation in a void consisting of one Kr atom and about ten vacancies. Unlike in the calculations of Hansen *et al.*, we observe the lifetimes to continue increasing beyond the 13-atom-vacancy complex. Extrapolation of the curve in Fig. 4(c) indicates that the lifetimes would saturate beyond a 20-atom-vacancy complex decorated with Kr.

The 260-ps lifetime in Cu irradiated with Kr can also arise from positrons trapped in a clean 3-atom-vacancy cluster. Our assignment of the 260-ps lifetime to a 9-vacancy Kr-decorated cluster is due to the assumption that the high dose of Kr irradiation saturates all vacancy clusters. Only annealing studies of Cu containing clean voids (e.g., produced by electron irradiation) and Kr-decorated voids can distinguish between the probable source of positron traps.

We now present the results of positron annihilation in clean and He-decorated vacancy complexes in Al. In Fig. 5 we plot the electron and positron density distribution in a clean and He-decorated monovacancy cluster. These results are qualitatively similar to those in Figs. 1—3. The variation of positron binding energy, positron fraction inside the void, and lifetime with void size in Al are given in Fig. 6. The increase in the binding energy with void size is due to the removal of the repulsive positive-ion core as in the case of Cu. The binding energy for a given void size in Al is, however, larger than that in Cu. This arises because Al is polyvalent (charge on the ion is +3), where as Cu is monovalent. As He decorates the void the positron binding is reduced. Consequently there is a significant drop in the positron lifetime.

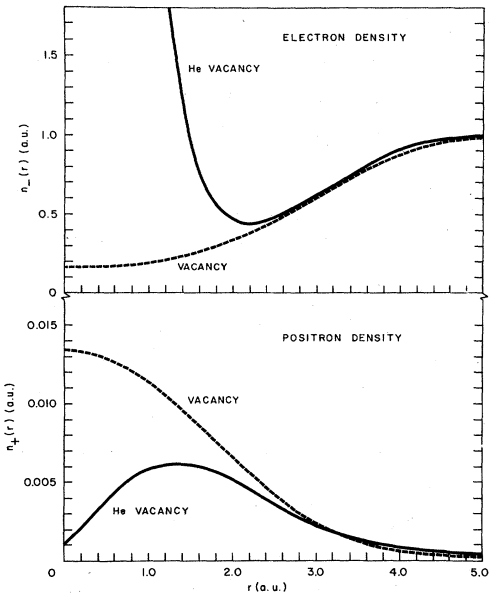

FIG. 5. Electron and positron density distribution around a monovacancy (dotted curve) and monovacancy-He complex (solid curve) in Al.

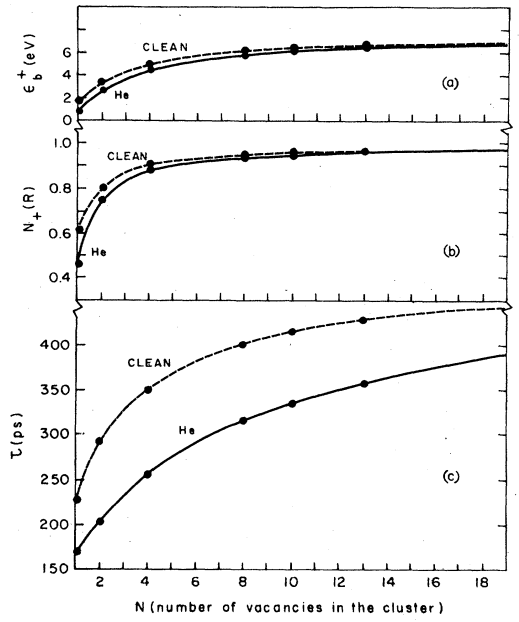

FIG. 6. Variation of (a) positron binding energy, (b) positron fraction inside the void, and (c) positron lifetime with void size in Al. In each case, the dashed curve corresponds to clean voids while the solid line corresponds to He-decorated voids.

TABLE IV. Positron binding energies and lifetimes calculated in the noninteracting atom model (Ref. 6) and jellium model (present calculation) in microvoids in Al.

No. of vacancies in the cluster	Condition	Present result ϵ_b (eV)	Present result τ (ps)	Ref. 6 ϵ_b (eV)	Ref. 6 τ (ps)
2	Clean	3.39	292	3.3	273
	He-decorated	2.67	205		
4	Clean	4.96	351	4.9	329
	He-decorated	4.45	256		
1	Clean	1.80	239	2.3	253
	He-decorated	0.86	172	1.7	191

Recently Hansen *et al.*[1] have measured positron lifetimes in α-irradiated Al. These authors observed that the long-lifetime component increased from 360 to 450 ps during annealing. Comparing this with the results in Fig. 6, we conclude that the 350-ps lifetime originates from positrons annihilating inside a He-12-vacancy cluster. This lifetime can also arise from positrons trapped inside a clean 5-vacancy cluster in Al. As discussed before in the case of *Cu*Kr system, we are assuming that all voids are saturated with He. It is also possible that large vacancy clusters may have variable shapes, and hence, a distribution of lifetimes, thus adding to the ambiguity of assignment of a given positron lifetime to a specific vacancy structure. Since our calculations (based upon spherical void structures) are in reasonable agreement with those of Hansen *et al.* (based upon real void structure), we believe that the variable shapes of a large void would not have a significant effect on positron lifetimes. Annealing studies are expected to help in the identification of positron traps. Furthermore, the prediction of the exact number of vacancies in the cluster has to be regarded with caution since various theoretical models predict lifetimes that can be different from each other by about 20 ps. To illustrate this we compare in Table IV the present positron lifetimes and binding energies in vacancy clusters and He-vacancy complex with those calculated by Puska and Nieminen.[6] The nature of agreement is similar to that discussed earlier in Tables II and III.

We now discuss the angular correlation between the photons produced during positron annihilation. The results for monovacancy and He-decorated monovacancy in Al are shown in Fig. 7. Note that peak counting rate in the He-decorated vacancy is about 5% less than in the monovacancy. Since these curves are normalized to equal areas, the full width at half maximum (FWHM) in the He-decorated vacancy is larger than that in the vacancy. This indicates that the positrons annihilate with larger momentum components of the electrons in the He-decorated vacancy. This result is similar to that noted in the vacancy-hydrogen complex.[21] Thus angular correlation can also provide a signature of the impurity trapping by vacancy complexes.

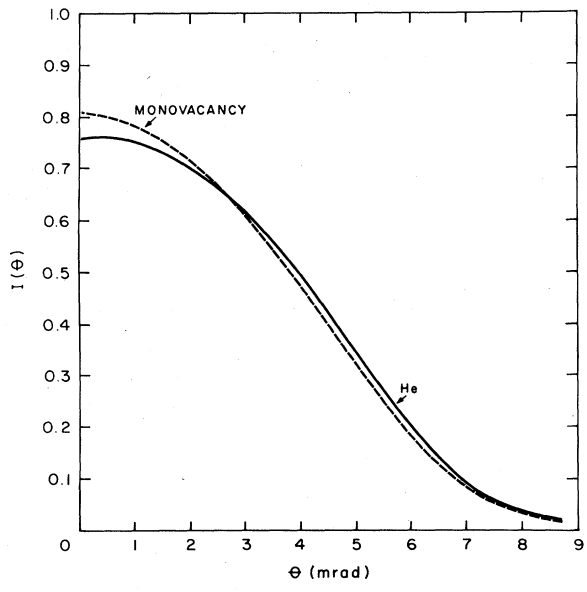

FIG. 7. Angular correlation curves for positron annihilation inside a monovacancy and He-decorated monovacancy in Al.

IV. CONCLUSIONS

Using the jellium model we have calculated the electronic structure of microvoids decorated with rare-gas atoms in fcc Al and Cu. The trapping of positrons in these vacancy-impurity complexes were studied by solving the positron Schrödinger equation. In our calculations the response of conduction electrons to the vacancy-impurity complexes was studied self-consistently using density-functional formalism. Our results were compared with other theoretical models. In particular, the results of the superposition atom model (where the discreteness of the lattice is taken into account but the charge redistribution around defect complexes is ignored) are in reasonable agreement with ours. Since these two models represent two extreme viewpoints, our comparison in Tables II, III, and IV indicate that the lifetimes for impurity-decorated or clean microvoid can be predicted within an accuracy of about 20 ps. With this reservation in mind, the calculated lifetimes as a function of void size can be compared with experimental measurements in irradiated materials to predict the predominant size of voids that trap the positron. From this one can then calculate the density of rare-gas atoms in the bubbles. Since these problems have

a great deal of technological importance, it is hoped that more experiments and theoretical investigations will be carried out. This will be useful in illustrating the role of positron annihilation as a probe of small impurity-void complexes. It will also be desirable to perform theoretical calculations for decorated voids where both electronic perturbation and discreteness of the lattice are preserved. For transition metal hosts, tight-binding calculations based upon the moment-expansion technique may prove to be useful since one can treat a larger number of atoms in the cluster. We are presently investigating such a program.

ACKNOWLEDGMENTS

This work was supported in part by grants from Thomas F. Jeffress and Kate Miller Jeffress Trust, National Science Foundation Grant No. INT-8306590 and by the Research Corporation. Generous support of the Academic Computing Staff at Virginia Commonwealth University is gratefully acknowledged.

---

*Permanent address: Institute of Physics, Sachivalaya Marg, Bhubaneswar 751005, India.

[1]H. E. Hansen, H. Rajainmäki, R. Talja, M. D. Bentzon, and R. M. Nieminen (unpublished).

[2]A. Magerl, J. J. Rush, J. M. Rowe, D. Richter, and H. Wipf, Phys. Rev. B **27**, 927 (1983).

[3]*Positrons in Solids in Current Trends in Physics,* edited by P. Hautojärvi (Springer, Heidelberg, 1979), Vol. 12.

[4]P. Jena, in *Treatise on Materials Science and Technology,* edited by F. Y. Fradin (Academic, New York, 1981), p. 351.

[5]M. Eldrup and J. H. Evans, J. Phys. F **12**, 1265 (1982).

[6]M. J. Puska and R. M. Nieminen, J. Phys. F **13**, 333 (1983).

[7]W. Brandt and J. Reinheimer, Phys. Lett. **35A**, 109 (1971).

[8]E. Bonderup, J. U. Andersen, and D. N. Lowy, Phys. Rev. B **20**, 883 (1979).

[9]T. M. Hall, A. N. Goland, and C. L. Snead, Phys. Rev. B **10**, 3062 (1974); P. Hautojärvi and P. Jauho, Acta Polytech. Scand. Phys. Incl. Nucleon. Ser. **98**, 1 (1973); M. J. Fluss, L. C. Smedskjaer, M. K. Chason, D. G. Legnini, and R. W. Siegel, Phys. Rev. B **17**, 3444 (1978).

[10]P. Hohenberg and W. Kohn, Phys. Rev. **136**, B864 (1964); W. Kohn and L. J. Sham, *ibid.* **140**, A1133 (1965).

[11]M. J. Stott and P. Kubica, Phys. Rev. B **11**, 1 (1975).

[12]C. H. Hodges and M. J. Stott, Phys. Rev. B **7**, 73 (1973).

[13]C. H. Hodges, Phys. Rev. Lett. **25**, 284 (1970).

[14]J. Arponen, P. Hautojärvi, R. Nieminen, and E. Pajanne, J. Phys. F **3**, 2092 (1973).

[15]M. Manninen, R. Nieminen, P. Hautojärvi, and J. Arponen, Phys. Rev. B **12**, 4012 (1975).

[16]R. P. Gupta, and R. W. Siegel, Phys. Rev. B **22**, 4572 (1980).

[17]B. Chakraborty and R. W. Siegel, Phys. Rev. B **27**, 4535 (1983).

[18]K. Iyakutti, J. L. Calais, and A. H. Tang Kai, J. Phys. F **13**, 1 (1983).

[19]T. McMullen, R. J. Douglas, N. Etherington, B. T. A. McKee, A. T. Stewart, and E. Zaremba, J. Phys. F **11**, 1435 (1981).

[20]H. E. Hansen, R. M. Nieminen, and M. J. Puska, J. Phys. F **14**, 1299 (1984).

[21]P. Jena, M. J. Ponnambalam, and M. Manninen, Phys. Rev. B **24**, 2884 (1981).